JOURNAL OF CATALYSIS 82, 457–468 (1983)

Benzene Hydrogenation over Iron

II. Reaction Model over Unsupported and Supported Catalysts

KI J. YOON AND M. ALBERT VANNICE

The Pennsylvania State University, Department of Chemical Engineering, University Park, Pennsylvania 16802

Received January 17, 1983

The kinetic behavior of unsupported iron and iron dispersed on η-Al_2O_3, SiO_2, carbon, and B-doped carbon in the benzene hydrogenation reaction was studied over a range of 390–515°K, 300–700 Torr H_2, and 15–100 Torr benzene in a differential, plug-flow reactor. Iron surface areas were measured by CO chemisorption, and turnover frequencies (TOF) over iron were found to be at least 10-fold lower than TOF values on the other Group VIII metals. These iron catalysts showed a maximum in activity vs temperature with all catalysts exhibiting this maximum near 473°K, except for unsupported iron for which it occurred at 493°K. Pressure dependencies on H_2 were consistently close to 3rd order whereas benzene pressure dependencies were temperature-dependent and varied between 0 and −1. A Langmuir–Hinshelwood rate expression of the form $r = k'P_{H_2}{}^3 P_B/(1 + K_BP_B)^2$ was found to provide a surprisingly satisfactory fit of all the data. In addition, this rate equation predicted the observed activity maximum and provided an explanation of this behavior which has also been observed in benzene hydrogenation over other metals. Values of enthalpy and entropy of adsorption for benzene which were obtained from the optimized rate equation were very reasonable and consistent. This study provided evidence that this reaction is structure insensitive over iron. No major support effect was found on kinetic behavior; however, iron dispersed on graphitized carbon and B-doped graphitized carbon exhibited superior activity maintenance and the maximum TOF values achievable were 2–5 times higher on the B-doped catalysts than on any other catalyst.

INTRODUCTION

Many studies have been conducted on benzene hydrogenation over Group VIII metals; however, most have concentrated on the more active metals such as Ni, Pt, and Pd, and few have been made on iron. Early studies indicated that iron had little or no activity in this reaction (*1, 2*), but subsequent investigations established that benzene could be hydrogenated on clean iron surfaces (*3–9*). These studies have dealt with iron films (*3, 7, 8*), iron powder, (*5, 6*), promoted iron (*5, 9*), and silica-supported iron (*4*). However, only the work of Phillips and co-workers has been directed toward a thorough characterization of the kinetic behavior, but this study was conducted on singly promoted iron (*9*).

This investigation was initiated to determine specific activities for benzene hydrogenation and to characterize the kinetic behavior of both unpromoted, unsupported iron and iron dispersed on Al_2O_3, SiO_2, carbon, and doped carbon supports. Any influence of the support and of iron crystallite size on catalytic behavior was also to be examined. The benzene reaction is of some current interest as it is the simplest model reaction which can be used to characterize catalysts for the upgrading of aromatic hydrocarbons obtained from coal liquefaction processes, and the availability of inexpensive catalysts would be very beneficial. Of particular interest in this study was the use of carbon doped with acceptor (B) and donor (K) elements to see if significant changes could be induced in the supported iron systems. The relative activities of these various catalysts and their activity maintenance behavior has been described in another paper (*10*). This paper discusses

0021-9517/83 $3.00

the kinetic behavior in detail and the reaction mechanism proposed to explain the results.

EXPERIMENTAL

Catalyst preparation. The catalysts in Table 1 were prepared using an incipient wetness technique in which only enough aqueous solution of $Fe(NO_3)_3 \cdot 9H_2O$ (Reagent grade—Fisher Sci.) to fill the pore volume was used. Details are provided elsewhere (*10*). The support materials utilized were: SiO_2 (Cab-O-Sil, Grade M5, Cabot Corp.), η-Al_2O_3 (from Exxon Research & Engr. Co.), Carbolac-1 (C-1) (Cabot Corp.), graphitized Vulcan 3 carbon (V3G) (Cabot Corp., and Ref. (*11*)), Monarch 700 carbon (MC) (Cabot Corp.), and graphitized Monarch 700 (GMC) (Ref. (*12*)). The boron-doped GMC supports were prepared by adding a solution of boric acid to a GMC sample, drying at 393°K, and heating under flowing Ar at 2073°K for 1 h (BC-11, 1%B), or at 2773°K for 0.25 h (BC-12, 1%B), or at 2773°K for 1 h (BC-1,0.1%B). Additional details are provided elsewhere (*12*). The iron/K-doped glassy carbon sample (3.4% Fe/K-GC) contained 0.09% K and was prepared using a recipe for monolithic glassy carbons (*13*). The two unsupported iron samples were ultrapure Fe_2O_3 powder and ultrapure Fe powder (<4 ppm impurities) obtained from Johnson Matthey Chem. Ltd.

Adsorption measurements. Volumetric adsorption measurements were conducted in a glass, Hg-free system capable of attaining vacuums to 10^{-6} Torr (1.3×10^{-4} Pa) using liquid N_2 traps. Details are given elsewhere (*14*). Hydrogen (Airco—99.999%) was further purified by passage through a Deoxo unit (Englehard Ind.), a 5-Å molecular sieve trap, and an Oxytrap (Alltech Assoc.). Carbon monoxide (Matheson grade—99.99%) was passed through a molecular sieve trap held at 373°K. Helium (Airco—99.9999%) was passed through a gas purifier (Alltech Assoc.), a molecular sieve trap, and an Oxytrap.

TABLE 1

Average Fe Crystallite Sizes, Activities, and Benzene Turnover Frequencies for Iron Catalysts

Catalyst	CO uptake (μmol/g cat)	$\bar{d}_s$ (nm)	Activity at 393°K[a] (μmol Bz · s^{-1} g cat^{-1})	TOF (molecules Bz · s^{-1} · $Fe_s^{-1} \times 10^3$)[a]			E_{app} (kcal · mol^{-1})
				393°K	448°K	473°K (maximum TOF)	
3.4% Fe/K-GC	105	2.2	Nil	—	—	—	—
5.0% Fe/C-1	160	2.2	0.30	0.93	—	—	—
10.0% Fe/Al_2O_3(2)	115	5.9	0.77	3.2	5.6	5.7	11 ± 2
4.8% Fe/GMC	27.5	12	0.012	0.22	8.0	15	23 ± 1
4.8% Fe/MC	26.0	12	—	—	3.8	7.8	27 ± 2
5.3% Fe/BC-11(2)	27.0	13	0.022	0.41	12.0	26	23 ± 2
4.8% Fe/BC-1	21.5	15	—	—	8.2	8.9	—
5.2% Fe/BC-12	22.0	17	—	—	20.0	26	23 ± 1
5.8% Fe/SiO_2	10.5	37	—	—	11.0	16	22 ± 3
4.5% Fe/V3G	5.6	54	—	—	6.1	8	17 ± 2
Reduced Fe_2O_3	6.8	990	—	—	1.6	5.2[d]	26 ± 3
Fe powder	1.0	6700	0.0013	0.65	15.0	—	20 ± 6
Al_2O_3-promoted Fe	—	60[b]	0.019[c]	0.12[c]	36[c]		~20

[a] P_{H_2} = 680 Torr, P_{Bz} = 50 Torr.
[b] Estimated from BET measurement in Ref. (9).
[c] Estimated by extrapolation of rate equation in Ref. (9).
[d] T = 493°K.

The technique of Emmett and Brunauer was used which involves the measurement of a CO isotherm at 195°K, evacuation for 2 min, and the measurement of a second isotherm (*15*). The difference between these two isotherms at pressures above 100 Torr has been found to be an accurate measure of reduced iron surface area (*10, 16 17*). The catalyst pretreatment involved slow heating in flowing H_2 to 673°K, reduction at this temperature for 16 h, and evacuation at 648°K for 30 min prior to adsorption measurements (*10*).

Kinetic measurements. The catalytic behavior of these samples for vapor-phase benzene hydrogenation was determined in a differential, plug-flow reactor system using small amounts of catalyst; i.e., typically about 0.3 g for supported catalysts and 2–5 g for unsupported iron. The liquid benzene was pumped to a preheater column using a miniature peristaltic pump (Rainin Instr.) with Viton tubing and an operating range of 0.002 to 1.0 cm^3 min^{-1}. The glass reactor was heated in a fluidized sandbath (Techne Inc.) capable of temperature control within ±0.2°K. The system was operated at atmospheric pressure (96–100 kPa), line pressures were measured with a transducer (Validyne Eng. Corp.), and gas flow rates were monitored using calibrated mass flowmeters (Teledyne Hasting–Raydist). Exit gas analyses were conducted with a gas chromatograph (Model 700-00, Hewlett–Packard) using 6-ft. columns packed with GP 10% 1,2,3-tris (2-cyanoethoxy) propane on 100/120 Chromosorb P AW (Supelco, Inc.) and He as a carrier gas. It was calibrated using benzene, cyclohexene, and cyclohexane. An electronic integrator (H–P 3390A) was used to determine peak areas. Additional details have been given elsewhere (*10*).

In this system, the H_2 was flowed through a 5-Å molecular sieve trap and an Oxytrap, and the He was passed through a gas purifier and an Oxytrap. The benzene samples, HPLC grade 99.9% purity and Ultrex grade 99.99%, were obtained from J. T. Baker Co., and were degassed by several freeze–thaw cycles conducted in a glove bag under He. They were then stored and used in this glove bag under flowing He to prevent any air from absorbing into the benzene.

The activity dependence on temperature was first measured at standard conditions (680 Torr H_2 and 50 Torr Bz) then partial pressure dependencies at different temperatures were determined. Flow rates of 20–50 cm^3 min^{-1} for H_2 and 0.005–0.02 cm^3 liquid min^{-1} (1–6 cm^3 vapor (STP) min^{-1}) for benzene were used with He providing the remainder, if necessary. Space velocities of 1000 to 3000 h^{-1} provided conversions between 0.1 and 5%. The same standard pretreatment was used; i.e., stepwise heating in flowing H_2 to 673°K and reduction at 673°K for 16 h prior to cooling in H_2 to the desired temperature.

Because of the slow activity loss which usually occurred during the days required to characterize each catalyst sample, methods had to be developed to correct the different sets of data for deactivation. A bracketing technique was used for all catalysts, except 10% Fe/Al_2O_3, which consisted of a 20-min exposure to pure hydrogen after every activity measurement, which was made after 20 min on-stream at the desired reaction conditions. Between sets of data, each of which was obtained in 1 day, the catalyst was kept under flowing H_2. For nearly all the catalysts this procedure was satisfactory to eliminate deactivation within a set of runs, and stable activity could be checked within a set by repeating various conditions. Each set was characterized at or near a standard set of reaction conditions of 680 Torr H_2 and 50 Torr benzene at a given temperature. This provided a correction factor for deactivation for that set of data. In some cases, deactivation was extremely slow and here the small corrections needed were obtained by measuring initial and final activities and assuming activity loss was proportional to time on-stream. The 5.0% Fe/C-1 and iron powder

catalysts deactivated too rapidly for meaningful kinetic studies and, in addition, they could not be regenerated completely by the standard pretreatment. The 10% Fe/Al_2O_3 also showed significant deactivation, but it could be completely regenerated by a 1-h reduction in H_2 at 673°K; therefore, this catalyst was subjected to this regeneration step after *every activity measurement* in the kinetic study. Very reproducible activities were obtained with this procedure.

RESULTS

The initial irreversible CO uptakes at 195°K and 200 Torr are listed in Table 1. Iron crystallite sizes were also calculated from x-ray line-broadening measurements and have been reported elsewhere (*10*). Only the chemisorption results are reported here because it is believed they provide a more accurate measure of crystallite size. A representative set of CO isotherms is shown in Fig. 1. The crystallite sizes were calculated assuming an adsorption stoichiometry of $CO_{(ad)}/Fe_s$ of $\frac{1}{2}$, where F_s is a surface Fe atom, and using

$$\bar{d}_s(\text{nm}) = 0.75/D$$

where $\bar{d}_s$ is the average crystallite diameter and D is metal dispersion (fraction exposed) (*17*). The initial activities are listed and the turnover frequency, TOF, is based upon initial dispersion values.

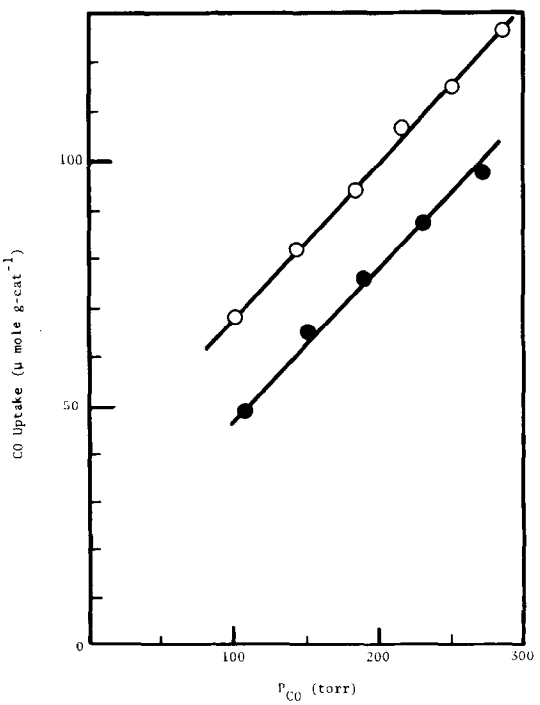

FIG. 1. CO adsorption on 5.2% Fe/BC-12 at 195°K; 1st CO (○), 2nd CO (●).

All catalysts showed a maximum in activity very close to 473°K, with the exception of the reduced Fe_2O_3 powder where the maximum was close to 493°K, and Fig. 2 shows typical activity–temperature relationships. Such behavior was also found with singly promoted iron, but the maximum occurred near 453°K (*9*). For this reason, apparent activation energies, E_{app}, were determined only in the low-temperature region between 390 and 450°K. These values are listed in Table 1 and most were near 22 ± 5 kcal mol^{-1} (1 cal = 4.184 J). For the partial pressure studies, a power rate law of the form $r = kP_{H_2}{}^X P_B{}^Y$ was initially used to determine exponential dependencies. At a given temperature, this routinely provided an excellent fit for hydrogen as shown in Fig. 3; however, the dependence always increased as temperature increased as indicated in Table 2. Regardless, most values were usually near 3 with the exception of the 10% Fe/Al_2O_3 catalyst. Log–log plots of rate versus P_B were not linear, as shown in Figs. 4 and 5; and the exponential dependences listed in Table 2 are only approximations in the higher P_B region. Nevertheless, they still provide a relative comparison of benzene pressure dependence at a given temperature and indicate a trend to less negative values as temperature increases. All catalysts are quite consistent in behavior except again for 10% Fe/Al_2O_3. Cyclohexane was the only product found over the entire conversion range.

DISCUSSION

Among the Group VIII metals, iron is known to have very low activity for benzene hydrogenation. This study confirms

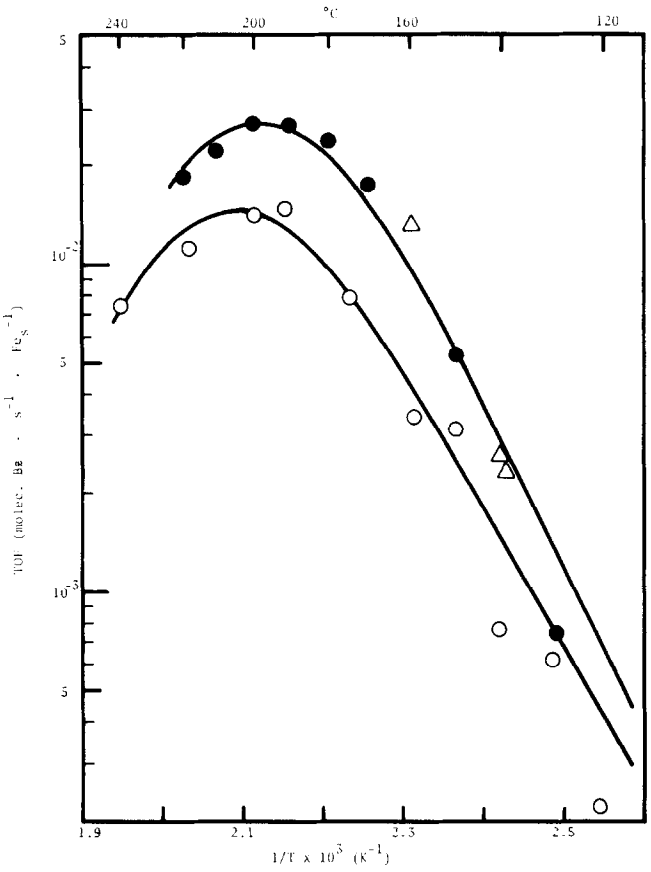

FIG. 2. Turnover frequency versus temperature for iron catalysts; P_{H_2} = 680 Torr, P_B = 50 Torr: 4.8% Fe/GMC (○), 5.2% Fe/BC-12: Set I (△), Set II (●). Solid lines represent predicted behavior using parameters in Table 5.

this and establishes that turnover frequencies on iron are at least an order of magnitude lower than TOF values on the other Group VIII metals under the reaction conditions employed here. A compilation of TOF values and kinetic parameters are given in Table 3 for comparison with the values for iron in Table 1, column 5, and in Table 2. The iron catalysts appear to be unique with their high apparent activation energies, a H_2 pressure dependence near 3, and negative benzene pressure dependencies. Only the 10% Fe/Al_2O_3 has kinetic parameters similar to those on other metals. However, as temperature increases, X values on these other metals increase and approach 3. In addition, the activity maximum observed for iron is not unique and similar maxima near 473°K have been observed on Ni (*20*), Pt (*27*), Re (*27*), Tc (*27*), and previously for iron (*9*). These maxima are not due to: (1) thermodynamic limitations, as equilibrium benzene conversion at 473°K at these conditions is above 99%; or (2) poisoning, as the maximum is traversed with both ascending and descending temperatures; or (3) diffusion effects, as at these low conversions and TOF values the Weisz criterion shows kinetic rates to be unimpeded by diffusion (*34*). As will be shown later, this behavior, which as yet has not been explained (*9*), is almost certainly due to a marked decrease in surface coverage of benzene as temperature increases which at some point is severe enough to decrease the overall rate.

TABLE 2

Partial Pressure Dependences Over Iron Catalysts Estimated Using $r = kP_{H_2}{}^X P_B{}^Y$

Catalyst	Sample	X				Y				
		413°K	433°K	448°K	473°K	413°K	433°K	448°K	474°K	493°K
10% Fe/Al_2O_3	2	0.5[a]	—	—	—	0.6[a]	—	—	—	—
		0.9[b]	—	1.6	—	0.2[b]	—	−0.5	—	—
4.8% Fe/GMC		3.2	—	3.8	4.0	−0.7	—	−0.4	−0.3	−0.4
5.3% Fe/BC-11	1	2.5	3.0	3.3	3.3	−0.7	−0.6	−0.6	−0.4[c]	—
5.3% Fe/BC-11	2	—	3.4	4.0	—	—	−0.8	−0.7[d]	—	—
5.2% Fe/BC-12		—	2.7	3.1	4.0	—	−0.7	−0.6	−0.6	—
5.8% Fe/SiO_2		—	—	4.0	—	—	−0.7	—	−0.2	−0.2
4.5% Fe/V3G		—	—	3.0	—	—	—	−0.4	—	—
Reduced Fe_2O_3		—	—	—	—	—	—	−1.0	−0.6	−0.3
Promoted Fe[e]		$X > 2$ (T = 403–453°K)				Y negative at higher P_B				

[a] T = 353°K.
[b] T = 393°K.
[c] T = 463°K.
[d] T = 453°K.
[e] From Ref. (9).

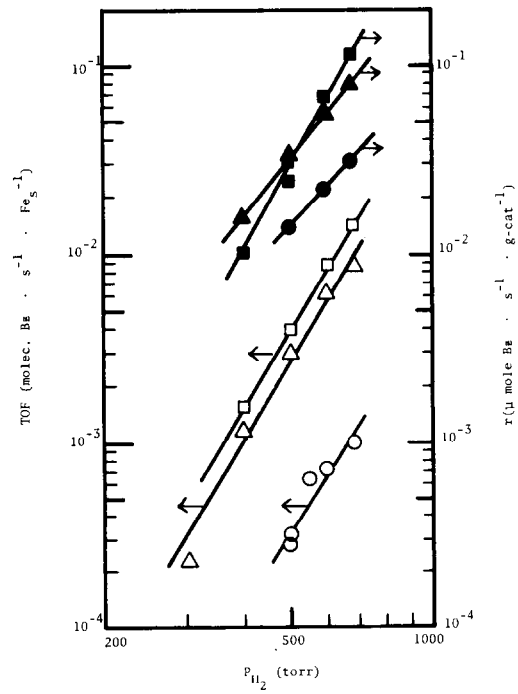

FIG. 3. Activity versus hydrogen pressure for iron catalysts; P_B = 50 Torr: 4.8% Fe/GMC: 413°K (○), 448°K (△), 473°K (□); 5.2% Fe/BC-12: 433°K (●), 448°K (▲), 473°K (■).

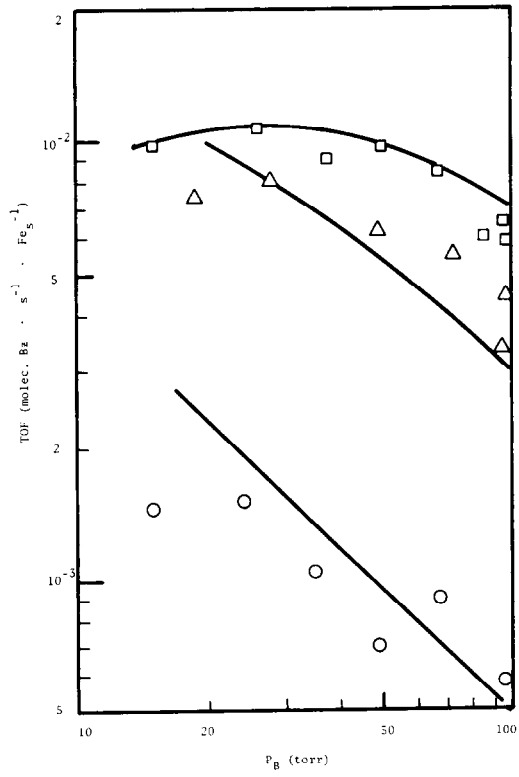

FIG. 4. Activity versus benzene pressure for 4.8% Fe/GMC; P_{H_2} = 600 Torr: 414°K (○), 448°K (△), 473°K (□). Solid lines represent predicted behavior using parameters in Table 5.

TABLE 3

Kinetic Behavior for Benzene Hydrogenation Over Group VIII Metals. Adjusted to Reaction Conditions of: Temp = 393°K, P_{H_2} = 680 Torr, P_B = 50 Torr.

Catalyst	TOF (molecules Bz · s^{-1} · $site^{-1}$ × 10^3)	$r = kP_{H_2}{}^X P_B{}^Y$		E_{app} (kcal mol^{-1})	Ref.
		X	Y		
(A) Fe					
Fe Film	0.022[a]	1[a]	0[a]	—	*8*
(B) Ni					
Ni crystal/SiO_2 (random orientation)	78[b]	1	[c]	—	*18*
Ni (111) face	30[b]	1	[c]	—	*18*
Ni (110) face	47[b]	1	[c]	—	*18*
Ni (100) face	28[b]	1	[c]	—	*18*
4–60% Ni/SiO_2	80	—	0.5	18.9	*19*
11.3% Ni/SiO_2	160	0.7	0.1	12.5	*20*
25% Ni/Al_2O_3	14	1.3	0.3	10.1	*21*
10% Ni/SiO_2	66	1.7	0.05	14	*22*
Ni/SiO_2, Al_2O_3, SiO_2–MgO	110	~1	0	14	*23*
67% Ni/kieselguhr	28	0.3	0.2	12	*24*
10% Ni/SiO_2	58	~2	~0.1	14	*25*
(C) Pt					
10% Pt/SiO_2	160–250	1.5	0	2.3	*22*
0.1–16% Pt/γ-Al_2O_3	1200	0.5	0	13	*26*
1% Pt/SiO_2	71[b]	—	—	8.0	*27*
Pt/SiO_2, Al_2O_3, SiO_2–MgO	280	~1	0	13	*23*
(D) Pd					
10% Pd/SiO_2 (Cab-O-Sil)	35[b]	—	—	11	*28*
0.5–25% Pd/SiO_2 (Davison)	7.4[b]	—	—	11	*28*
1% Pd/SiO_2	6.1[b]	—	—	9.5	*27*
Pd/SiO_2, Al_2O_3, SiO_2–MgO	16	1	0	14	*23*
0.2–1% Pd/Al_2O_3	35[b]	—	—	10	*29*
2% Pd/SiO_2, Al_2O_3, MgO	28[b]	—	—	9.5	*30*
(E) Co					
10% Co/SiO_2	22	1	0.2	5.8	*31*
10% Co/Al_2O_3	24	1	0.3	5.4	*31*
10% Co/carbon	20	1.5	0.2	1.2	*31*
Others					
Ru/SiO_2	160[b]	—	—	7.0	*27*
Ir/Al_2O_3	~550[b]	—	—	—	*32, 33*
Os/Al_2O_3	~200[b]	—	—	—	*33*

[a] Measured at 273°K; P_{H_2} = 20 Torr.
[b] Estimated by assuming E_{app} = 11 kcal mol^{-1}, X = 1, and Y = 0 if not specified.
[c] Slightly positive.

As mentioned earlier, a simple power rate law did not adequately describe the kinetic behavior exhibited by these iron catalysts, the most salient features of which were: an activity maximum near 473°K, a near 3rd-order dependence on H_2, and a benzene pressure dependence which increased from inverse 1st order to near zero order as temperature increased. Many different reaction models and rate equations were proposed and examined, but only one was consistent with all the data (*34*). This

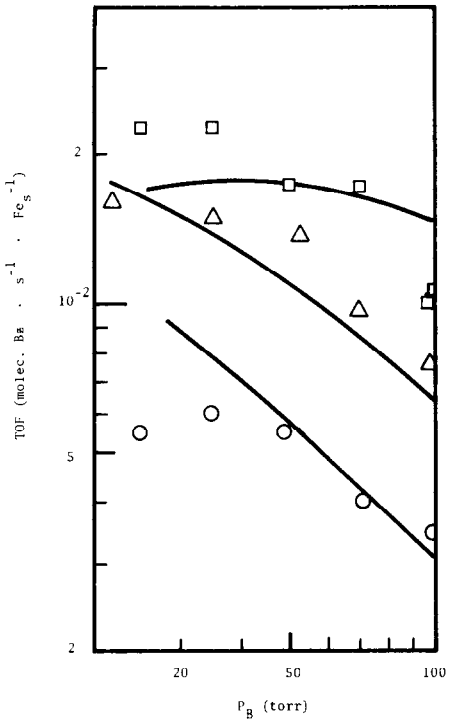

FIG. 5. Activity versus benzene pressure for 5.2% Fe/BC-12; P_{H_2} = 600 Torr: 433°K (○), 448°K (△), 473°K (□). Lines represent predicted behavior using parameters in Table 5.

was a Langmuir–Hinshelwood (L-H) rate expression of the form

$$r = \frac{kK_E K_B K_{H_2}{}^3 P_{H_2}{}^3 P_B}{(1 + K_B P_B)^2} = \frac{k' P_{H_2}{}^3 P_B}{(1 + K_B P_B)^2} \quad (1)$$

which can be derived from the following sequence of elementary steps

$$H_{2\,(g)} + 2S \overset{K_{H_2}}{\longleftrightarrow} 2H\text{–}S \quad (I)$$

$$C_6H_{6\,(g)} + S \overset{K_B}{\longleftrightarrow} C_6H_6\text{–}S \quad (II)$$

$$C_6H_6\text{–}S + 5H\text{–}S \overset{K_E}{\longleftrightarrow} C_6H_{11}\text{–}S + 5S \quad (III)$$

$$C_6H_{11}\text{–}S + H\text{–}S \overset{k}{\longrightarrow} C_6H_{12}\text{–}S + S \text{ (RDS)} \quad (IV)$$

$$C_6H_{12}\text{–}S \overset{1/K_C}{\longleftrightarrow} C_6H_{12\,(g)} + S \quad (V)$$

where K_{H_2}, K_B, and K_C are equilibrium adsorption constants for H_2, benzene, and cyclohexane, respectively, k is the rate constant in the rate determining step (RDS), and S represents a surface active site. It is worthwhile to note at this point that S may consist of a single metal atom or of an ensemble of atoms and, in addition, it may not necessarily be identical to the adsorption site detected by CO adsorption at 195°K. This equation is obtained in a straightforward manner subject to the assumptions listed in Table 4, some of which are implicit in L-H kinetics. Only the choice of the addition of the last H atom to a C_6H_{11} surface species provides a 3rd-order dependence on H_2 pressure simultaneously with the possibility of a benzene pressure dependence between 0 and −1. In addition to providing agreement with the experimental results, Assumption 5 in Table 4 is supported by the work of Badilla-Ohlbaum *et al.* (*9*), who found cyclohexane had no inhibiting effect, and the fact that hydrogen is typically more weakly bound than benzene on Group VIII metals, such as Ni (*26*) and Pt (*35*), for example. The measured X values which were significantly greater than 3 are presumed at this time to be a consequence of a deactivation process superimposed on the benzene hydrogenation reaction. This deactivation is enhanced at low H_2 pressures and higher temperatures, thereby producing an artificially high dependence on H_2. This deactivation appears to be due to the formation of surface carbo-

TABLE 4

Assumptions Employed for Derivation of L-H Rate Equation

1. Adsorbed benzene and adsorbed hydrogen are in equilibrium with the gas phase species
2. Benzene and hydrogen chemisorb competitively on the same type of active sites
3. Benzene chemisorbs associatively and occupies one active surface site
4. Hydrogen chemisorbs dissociatively and requires two sites
5. The surface coverages of hydrogen, partially hydrogenated benzene species, and cyclohexane are very small
6. The last hydrogen addition step on the surface is the rate determining step (RDS), and this step is irreversible

naceous species and/or carbide formation, and it has been discussed elsewhere (*10*).

Remembering that equilibrium adsorption constants can be written as

$$K_i = \exp(\Delta S_i^0/R - \Delta H_i^0/RT) \quad (2)$$

and the rate constant as

$$K = \exp(S\ddagger/R - H\ddagger/RT) \quad (3)$$

where ΔS_i^0 and ΔH_i^0 are the standard entropy and enthalpy of adsorption, respectively, and $S\ddagger$ and $H\ddagger$ are the entropy and enthalpy associated with the RDS, then from Equation (1) ΔH_C is defined as

$$\Delta H_C = H\ddagger + \Delta H_E + \Delta H_B{}^0 + 3\Delta H_{H_2}{}^0 \quad (4)$$

Equation (1) can be written

$$r = \text{TOF} = \frac{A' \exp(-\Delta H_C/RT) P_{H_2}{}^3 P_B}{[1 + \exp(\Delta S_B^\circ/R - \Delta H_B^\circ/RT) P_B]^2} \quad (5)$$

and it predicts a maximum in activity versus temperature, i.e.,

$$(\partial r/\partial T)_{T=T_{max}} = 0$$
$$= \Delta H_C[1 + \exp(\Delta S_B^\circ/R - \Delta H_B^\circ/RT_{max})P_B]$$
$$- 2P_B\Delta H_B^\circ \exp(\Delta S_B^\circ/R - \Delta H_B^\circ/RT_{max})P_B \quad (6)$$

Since TOF_{max} was known at T_{max}, four unknown parameters, A', ΔH_C, ΔS_B°, and ΔH_B° existed. Initial reasonable estimates for ΔS_B° and ΔH_B° could be made, and then a trial-and-error procedure using an Apple II Plus computer was employed to find values of A' and ΔH_C which gave the best fit of activity versus temperature plus activity versus P_B at the various temperatures. A range of ΔS_B° and ΔH_B° values were covered and the optimum values obtained in this manner are listed in Table 5. The predicted rates are shown in Figs. 4 and 5 by the solid lines. Although not perfect, extremely satisfactory fits were obtained considering the complexity of the kinetic behavior, especially in describing the activity versus temperature.

The appearance of the activity maximum over these metals can now be explained. At lower temperatures, the K_BP_B term dominates in the denominator, the rate simplifies to $k'P_{H_2}{}^3/K_B{}^2P_B$ and the apparent activation energy $E_{app} = \Delta H_C - 2\Delta H_B^\circ$. The agreement between observed and predicted values shown in Table 5 is not exact, but is quite close, and the trends in high and low E_{app} values are certainly followed. Better agreement in E_{app} could have been obtained, but the curves in Figs. 4 and 5 would have shown greater disparity. Because adsorption is exothermic, K_B decreases with increasing T and in some region K_BP_B will become negligible compared to 1. In this case, $E_{app} = \Delta H_C$ and it can be negative if $(\Delta H_B^\circ + 3\Delta H_{H_2}^\circ)$, which must be negative, is larger in absolute value than

TABLE 5

Optimized Kinetic Parameter Values for Iron Catalysts

Catalyst	Sample	A' (Bz molec. s^{-1} Fe_s^{-1} atm^{-4})	ΔH_C (kcal mol^{-1})	ΔH_B° (kcal mol^{-1})	ΔS_B° (e.u.)	E_{app} (kcal mol^{-1})	
						Predicted	Obs.
4.8% Fe/GMC		3.02×10^{-13}	−28	−24	−44	20	23
5.3% Fe/BC-11	1	7.56×10^{-12}	−24	−21	−38	18	15
5.3% Fe/BC-11	2	5.23×10^{-13}	−28	−24	−44	20	23
5.2% Fe/BC-12		3.17×10^{-13}	−28	−25	−47	22	23
5.8% Fe/SiO_2		6.86×10^{-12}	−25	−22	−40	19	22
4.5% Fe/V3G		3.78×10^{-9}	−18	−17	−30	16	17
Reduced Fe_2O_3		6.79×10^{-15}	−32	−27	−48	22	26

($H\ddagger + \Delta H_E$). In essence, θ_B is high at low T but decreases rapidly as T increases and finally becomes low enough to retard the rate; that is, $k' = kK_EK_BK_{H_2}{}^3$ and the $K_BK_{H_2}{}^3$ terms dominate and decrease k' as T increases. The location of T_{max} was very reproducible for these supported catalysts regardless of differences in specific activity greater than 1 order of magnitude. This is strong evidence that the occurrence of the activity maximum is a phenomenon attributable to the kinetics of the reaction rather than a thermal artifact, and it infers that isothermal conditions existed in each kinetic measurement. This explanation is supported by the previous study on iron, where the activity maximum occurred at 453°K at much lower benzene pressures (below 3 Torr). The decrease in θ_B should occur at a lower temperature at lower P_B values.

If this equation has meaning in the Langmuirian sense, then the equilibrium adsorption constants must contain ΔS_i° and ΔH_i° values which are physically reasonable (*36, 37*). In short, both ΔS_i° and ΔH_i° must be negative and $|\Delta S_i^\circ|$ must be smaller than the total entropy of the molecule and, in addition, ΔS_i° is also expected to satisfy the guidelines indicated by the equation below (*36, 37*)

$$10 \text{ e.u.} \leq -\Delta S_i^\circ \leq 12.2 - 0.0014\,\Delta H_B^\circ. \quad (7)$$

Because values of $S_{B(g)}^\circ$ lie between 72 and 80 e.u. (cal mol^{-1} K$^{\circ-1}$) at 390–515°K (*38*), the first two absolute criteria are satisfied. An examination of the values in Table 5 finds that the last two guidelines are also met. The consistency of the ΔH_B° and ΔS_B° values, excluding the possible deviation of 4.5% Fe/V3G, is certainly worth noting. Heat of adsorption data for benzene on iron were searched for but none was found; however, values of ΔH_B° of -30 and -12 kcal mol^{-1} have been reported for nickel (*39, 40*) indicating that these optimal calculated values are very reasonable. Entropy of adsorption values for benzene on nickel have been calculated from statistical thermodynamics and found to be -33 e.u. for mobile adsorption and -47 e.u. for immobile adsorption (*20*). This also indicates that these optimum parameters are very reasonable.

This model seems more satisfying than the one proposed by Badilla-Ohlbaum *et al.* for several reasons. First, it involves only a two-body collision on the surface rather than a seven-body collision, which is very improbable in a rate determining step. Second, the $\Delta H_{H_2}^\circ$ and ΔH_B° values of -2.3 and -6.85 kcal mol^{-1}, respectively, seem very low for heats of chemisorption and the $\Delta S_{H_2}^\circ$ and ΔS_B° values of -10.8 and -8.0 e.u. also seem rather low. Third, this model also allows for positive benzene dependencies and should be able to correlate the data in Ref. (*9*). A simple shift to a RDS involving a C_6H_x species with x less than 11 progressively shifts the H_2 pressure dependence to lower values. In fact, it may well be such a change in the RDS that is responsible for the distinctly different behavior of the 10% Fe/Al_2O_3 catalyst. Finally, this model provides a reasonable explanation for the activity decline which occurs at higher temperatures and eliminates the need to propose a different mechanism as suggested in the previous kinetic study (*9*).

Iron dispersed on graphitized carbon and B-doped carbons has been found to have much better activity maintenance than iron powder, Fe/Al_2O_3, and Fe/SiO_2 (*10*), and, as shown in Table 1, the highest TOF were obtained with the 1% B-doped carbon supports. However, no significant change in E_{app}, ΔS_B°, or ΔH_B° seems to occur for these B-doped catalysts and the same reaction sequence is applicable to all catalysts in Table 5. Only subtle changes would be needed, though, to increase TOF values two- to five-fold, and the major role of the boron, if any, may be to maintain a cleaner surface. The addition of potassium to the Fe-glassy carbon system was not beneficial, and it produced an effect opposite to boron in that the system either was initially inactive or it

deactivated completely within 20 min on-stream. Iron in the form of small crystallites (2.2 nm) also was an inferior catalyst because of its extremely rapid deactivation (*10*), and high dispersions did not produce improved catalysts for this reaction. However, the initial activities shown in Table 1 were very similar for all catalysts, with the exception of 10% Fe/Al_2O_3, indicating that benzene is a structure insensitive reaction. A comparison of TOF values at 448°K also supports this conclusion as no trend is discernable over a crystallite size range of 6–6700 nm; however, this size range is larger than that expected to produce significant structure sensitivity, were it to occur. In view of the overall performances of 4.8% Fe/GMC, 5.3% Fe/BC-11, and 5.2% Fe/BC-12, iron dispersed on graphitizied carbon and B-doped graphitized carbon represents the best iron catalysts for benzene hydrogenation.

SUMMARY

The kinetic behavior of unsupported iron and iron dispersed on η-Al_2O_3, SiO_2, carbon, and B-doped carbon in the benzene hydrogenation reaction was studied over a range of 390–515°K, 300–700 Torr H_2, and 15–100 Torr benzene in a differential, plug-flow reactor. Iron surface areas were measured by CO chemisorption and turnover frequencies over iron were found to be at least 10-fold lower than TOF values on the other Group VIII metals. These iron catalysts showed a maximum in activity versus temperature with all catalysts exhibiting a maximum at 473°K, except for unsupported iron for which it occurred at 493°K. Pressure dependencies on H_2 were consistently close to 3rd order whereas benzene pressure dependencies were temperature-dependent and varied between 0 and −1. One Langmuir–Hinshelwood rate expression of the form $TOF = k'P_{H_2}{}^3 P_B/(1 + K_B P_B)^2$ was found to provide a surprisingly satisfactory fit of all the data from this rather complicated behavior. In addition, this rate equation predicts an activity maximum and provides for an explanation of this behavior, which has also been observed in benzene hydrogenation over other metals. Very consistent and reasonable values for ΔS_B° and ΔH_B° were obtained which provided satisfactory fits of the data for all the catalysts studied. Evidence from this study indicates that this reaction is structure insensitive over iron. No major support effect was found on kinetic behavior; however, iron dispersed on graphitized carbon and B-doped graphitized carbon exhibited superior activity maintenance and the maximum TOF achievable were 2–5 times higher on the B-doped catalysts than on any other system.

ACKNOWLEDGMENTS

This research was supported by the NSF through Grant CPE-7915761. This grant was cosponsored by the Army Research Office.

REFERENCES

1. Emmett, P. H., and Skau, N., *J. Am. Chem. Soc.* **65,** 1029 (1943).
2. Long, J. H., Frazer, J. C. W., and Ott, E., *J. Am. Chem. Soc.* **56,** 1101 (1934).
3. Beeck, O., and Ritchie, A. W., *Discuss. Faraday Soc.* **8,** 159 (1950).
4. Schuit, G. C. A., and van Reijen, L. L., *in* "Advances in Catalysis" (D. D. Eley, W. G. Frankenburg, and V. I. Komarewsky, Eds.), Vol. 10, p. 243. Academic Press, New York, 1958.
5. Phillips, M. J., and Emmett, P. H., *Int. Congr. Pure Appl. Chem., 18th,* Paper B1-28, 1961.
6. Deberbentsev, Y. I., Paal, Z., and Tétényi, P., *Z. Phys. Chem. Neue Folge* **80,** 51 (1972).
7. Anderson, J. R., and Kemball, C., *in* "Advances in Catalysis" (D. D. Eley, W. G. Frankenburg, and V. I. Komarewsky, Eds.), Vol. 9, p. 51. Academic Press, New York, 1957.
8. James, R. G., and Moyes, R. B., *J. Chem. Soc. Faraday Trans. 1* **74,** 1666 (1978).
9. Badilla-Ohlbaum, R., Neuburg, H. J., Graydon, W. F., and Phillips, M. J., *J. Catal.* **47,** 273 (1977).
10. Yoon, K. J., Walker, P. L., Jr., Mulay, L. N., and Vannice, M. A., *I&EC Prod. Res. Dev.*, in press.
11. Jung, H-J., Walker, P. J., Jr., and Vannice, M. A., *J. Catal.* **75,** 416 (1982).
12. Rao, A. V. Prasad, and Mulay, L. N., to be published.

13. Moreno-Castilla, C., Mahajan, O. P., Walker, P. L., Jr., Jung, H-J., and Vannice, M. A., *Carbon* **18,** 271 (1980).
14. Palmer, M. B., and Vannice, M. A., *J. Chem. Technol. Biotechnol.* **30,** 205 (1980).
15. Emmett, P. H., and Brunauer, S., *J. Am. Chem. Soc.* **59,** 310 (1937); **59,** 1553 (1937).
16. Boudart, M., Delbouille, A., Dumesic, J. A., Khammouma, S., and Topsøe, H., *J. Catal.* **37,** 486 (1975).
17. Jung, H-J., Vannice, M. A., Mulay, L. N., Stanfield, R. M., and Delgass, W. N., *J. Catal.* **76,** 208 (1982).
18. Dalmai-Imelik, G., and Massardier, J., *Proc. Int. Congr. Catal. 6th,* **1,** 90 (1976).
19. Ione, K. G., Romannikov, V. N., Davydon, A. A., and Orlova, L. B., *J. Catal.* **57,** 126 (1979).
20. van Meerten, R. Z. C., and Coenen, J. W. E., *J. Catal.* **46,** 13 (1977).
21. Sica, A. M., Valles, E. M., and Giola, C. E., *J. Catal.* **51,** 115 (1978).
22. Taylor, W. F., *J. Catal.* **9,** 99 (1967).
23. Aben, P. C., Platteeuw, J. C., and Stouthamer, B., *Recl. Trav. Chim. Pays-Bas* **89,** 449 (1970).
24. Marangozis, J. K., Mantzouranis, B. G., and Sophos, A. N., *Ind. Eng. Chem. Prod. Res. Dev.* **18,** 61 (1979).
25. Taylor, W. F., and Staffin, H. K., *Trans. Faraday Soc.* **63,** 2309 (1967).
26. van Meerten, R. Z. C., Morales, A., Barbier, J., and Maurel, R., *J. Catal.* **58,** 43 (1979).
27. Kubicka, H., *J. Catal.* **12,** 223 (1968).
28. Moss, R. L., Pope, D., Davis, B. J., and Edwards, D. H., *J. Catal.* **58,** 206 (1979).
29. Gomez, R., Fuentes, S., Fernandez del Valic, F. J., Campero, A., and Ferreira, J. M., *J. Catal.* **38,** 47 (1975).
30. Figueras, F., Gomoz, R., and Primet, M., *Adv. Chem. Ser.* **121,** 480 (1973).
31. Taylor, W. F., and Staffin, H. K., *J. Phys. Chem.* **71,** 3314 (1967).
32. Brunelle, J. P., Montarnal, R. E., and Sugier, A. A., *Proc. Int. Congr. Catal. 6th, 1976* **2,** 844 (1976).
33. Betizeau, C., Leclercq, G., Maurel, R., Bolivar, C., Charcosset, H., Frety, R., and Tournayan, L., *J. Catal.* **45,** 179 (1976).
34. Yoon, K. J., Ph.D. thesis, The Pennsylvania State University, 1982.
35. Basset, J. M., Dalmai-Imelik, G., Primet, M., and Mutin, R., *J. Catal.* **37,** 22 (1975).
36. Boudart, M., Mears, D. E., and Vannice, M. A., *Ind. Chim. Belge* **32,** Special Issue, 281 (1967).
37. Vannice, M. A., Hyun, S. H., Kalpakci, B., and Liauh, W. C., *J. Catal.* **56,** 358 (1979).
38. Hougen, O. A., and Watson, K. M., "Chemical Process Principles," Part II, p. 527. Wiley, New York, 1947.
39. Bond, G. C., "Catalysis by Metals," Chap. 13. Academic Press, New York, 1962.
40. Tétényi, P., Babernics, L., Guczi, L., and Schächter, K., *Proc. Int. Congr. Catal. 3rd, 1964* 547 (1965).